Fractal pharmacokinetics of the drug mibefradil in the liver

J. Fuite, R. Marsh, and J. Tuszyński
Department of Physics, University of Alberta, Edmonton AB, T6G 2J1, Canada
(Received 23 April 2002; published 13 August 2002)

We explore the ramifications of the fractal geometry of the key organ for drug elimination, the liver, on pharmacokinetic data analysis. A formalism is developed for the use of a combination of well-stirred Euclidean and fractal compartments in the body. Perturbation analysis is carried out to obtain analytical solutions for the drug concentration time evolution. These results are then fitted to experimental data collected from clinically instrumented dogs [see, A. Skerjanec *et al.*, J. Pharm. Sci. **85**, 189 (1995)] using the drug mibefradil. The thus obtained spectral fractal dimension has a range of values that is consistent with the value found in independently performed ultrasound experiments on the liver.

DOI: 10.1103/PhysRevE.66.021904 PACS number(s): 82.39.−k, 05.45.Df, 61.43.Hv, 82.30.−b

I. INTRODUCTION

Pharmacokinetics is concerned with the quantification of the fate of a drug in the body [1]. It can reveal valuable information about the path of a drug, its volume of distribution, its metabolism, and elimination [2]. Traditionally, pharmacokinetic models involve compartmentalized systems, where the invasion and elimination of a drug from a particular compartment is modeled by a series of simple exponentials due to the governing first-order chemical kinetics approach [3].

The fundamental problem of pharmacokinetics is to mathematically describe the course of a drug through the body [4]. Conventionally, the spaces through which the drug travels are divided into compartments, and the invasion and elimination of the drug from each compartment are expressed in terms of the relevant kinetic rate constants. Any foreign substance introduced into the body appears in the blood and then passes to other tissues or fluids by simple diffusion until it is metabolized and/or eliminated. The extravascular compartments may include the gastrointestinal tract, the liver, urine, or sweat. Conventional pharmacokinetics treats the spaces through which a drug passes as individual compartments connected in series or parallel. Each compartment is typically envisioned as a homogeneous entity that represents an average state [5].

To understand the mechanics of a compartment model, we may look at the three-compartment example in Fig. 1, which depicts the movement of a drug injected into muscular interstitial tissue. From the muscle, the drug enters the blood and from there is reversibly transferred to the extravascular space. The kinetic coefficient k_{21} represents elimination from the first compartment, k_{02} represents excretion, and k_{23} and k_{32} represent rates of transfer. The indices denote the direction of transfer, so k_{21} indicates flow into the second compartment from the first while k_{23} indicates flow to compartment three from compartment two, etc.

Pharmacological data generally consists of concentration versus time measurements for each compartment. Typical curves for pure absorption and pure elimination after a bolus dose D_0 are shown schematically in Fig. 2(a). When there is simultaneous invasion and elimination, the combined concentration versus time curve takes the form given in Fig. 2(b). Initially, invasion is much larger than elimination, so the curve climbs steeply upward. Invasion then decreases while elimination increases until the two become equal, giving rise to the maximum compartment concentration. After the peak value, both absorption and elimination decrease and the curve slopes downwards. In the majority of cases, the constant of absorption is much higher than the constant of elimination, and the absorption rate becomes negligible after the peak [6]. Such a curve has been traditionally modeled by a sum of exponentials that works well for short to moderate times [6].

One problem with the traditional models is that they rely on the assumption of first-order kinetic processes, where each compartment is considered to be homogeneous, or ''well stirred.'' In other words, there is an instantaneous equilibrium reached after the appearance of the drug in a compartment. Numerous attempts to overcome this simplification have been made, including the development of parallel tube models, dispersive models, the incorporation of physiological attributes such as the perfusion of body tissues, and an *ad hoc* use of power functions of time [7,8]. Unfortunately, all these methods still have limitations [9]. Recently, however, it has been proposed that fractal theory may be applied to pharmacokinetics [9]. Although fractal kinetics has been studied for some time and has been applied to the flow of blood in the body [10–12], it was not until 1996 that the techniques of fractal analysis were applied to pharmacokinetics [9,13]. For example, Macheras [9] developed what he calls a homogeneous-heterogeneous distribution model based on the fractal properties of blood flow.

From a drug's site of administration, the blood is the predominant method of transport through the body to the drug's final destination. Conventionally, the blood is treated as a simple compartment, although the vascular system is highly

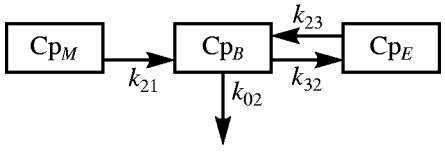

FIG. 1. Basic pharmacokinetic model for a drug that is absorbed into muscle, distributed, and eventually eliminated by the blood, but reversibly transferred to the extravascular space.

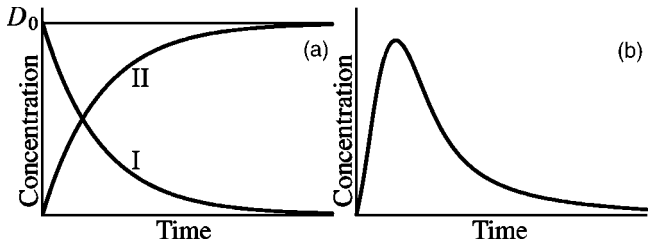

FIG. 2. Typical pure elimination (I) and pure invasion (II) curves. (b) Simultaneous invasion and elimination curve.

complex and consists of an estimated 96 000 km of vessels [14]. Recently, however, the fractal nature of the vascular network has been described, providing a simple way to take the complex geometry of the vascular system into account [15].

Numerous studies have been done to apply fractals to general kinetic theory [16–19], but surprisingly little work has been done on fractal pharmacokinetic theory [20,21], virtually none of it being quantitative. Consequently, the purpose of this paper is to investigate the application of fractal theory to pharmacokinetics. In addition to providing an experiment for the treatment of the liver as a fractal object, we develop here a practical kinetic description of the process of drug elimination from the bloodstream. To make the argument convincing we illustrate the model with an application to a particular data set that was collected by Skerjanec *et al.* [22] using the drug mibefradil on clinically instrumented dogs.

The objective of the first study performed by Skerjanec *et al.* [22] was to assess the suitability of mibefradil as a model for human pharmacokinetics. Mibefradil is a calcium antagonist currently being developed to reduce ventricular fibrillation [23,24]. Tam and co-workers found that, similar to drugs in humans, the kinetics of mibefradil in dogs becomes nonlinear with increasing oral dose. Skerjanec *et al.* [22] stated, however, that it was not possible to quantify the contribution of organs involved in presystemic metabolism and their role in the nonlinear kinetic behavior of mibefradil. To explore this nonlinearity further, Skerjanec *et al.* [22] performed a second, physiological study using four chronically instrumented female dogs ranging in weight from 19 to 24 kg. Three single oral doses of 1, 3, and 6 mg/kg each, a multiple oral dose treatment of 1.5 mg/kg every 12 h for eight days, and a 1 mg/kg for 10 min intravenous dose into the cephalic vein were administered to each dog in random order, with a one-week break between treatments. Blood samples were drawn from catheters placed in the jugular vein, coronary artery, hepatic vein, and portal vein, providing a series of plasma concentration versus time profiles. The hypothesized path of mibefradil through the body of the dog is depicted in Fig. 3. Note that there is a feedback loop into the liver via the aorta.

The results of the study by Skerjanec *et al.* [22] showed that the liver is the major site of drug elimination from the body. The conclusions of this study were that the nonlinear kinetics of mibefradil in dogs is mainly due to dose and time-dependent reduction of hepatic clearance. At present, the cause of this reduction is not known but several possibilities have been mentioned including nonlinear absorption and/or elimination, and product inhibition that can lead to dose and time-dependent changes in elimination kinetics. We believe that the fractal structure of the liver with the attendant kinetic properties of drug elimination may be responsible for some of the nonstandard behavior.

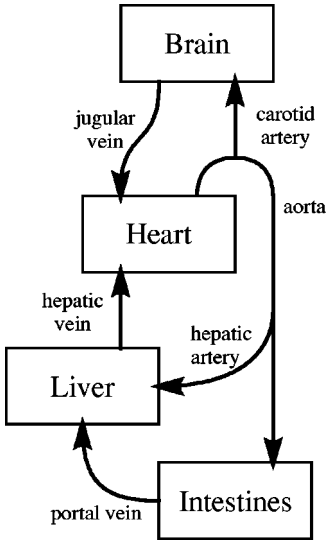

FIG. 3. Simplified diagram of the course of mibefradil through the body.

II. FRACTAL STRUCTURE OF THE LIVER

In an attempt to bring some aspects of physical analysis to bear on the study of the pharmacokinetics of mibefradil, the physical structure of the liver, the main site of the drug's metabolism [23,24] is selectively considered. It appears that in humans the liver is the largest visceral organ and it possesses unusual microcirculatory pathways [25]. It is supplied with blood by both the hepatic artery and the hepatic portal vein, thus being the first structure to receive xenobiotically laden blood from the intestines [26].

Elias [27] defines the liver as a continuous mass of parenchymal cells tunneled by vessels through which venous blood flows on its way from the gut to the heart. The circulation in the liver can be divided into the macrocirculation and the microcirculation. The former is comprised of the portal vein, hepatic artery, and hepatic veins, while the latter consists of the portal vein, hepatic arterioles, and the sinusoids [25]. The sinusoids are the specialized capillaries of the liver that form an uninterrupted three-dimensional network and are fully permeable to substances.

This macrocirculation spans the axes of the liver while branching into successively smaller vessels. At the anatomical level, there exist small histological units, called lobules, made up of an interlacing channel network of sinusoids supplied with blood and drug by the terminal ends of the portal venules and hepatic arterioles. Between the individual sinusoids of the interior of a lobule, one-cell-thick sheets of hepatocytes are interspersed [28,29]. Facing the blood spaces, the convoluted uptake surface of the hepatocytes expands the blood-tissue interface by the presence of numerous

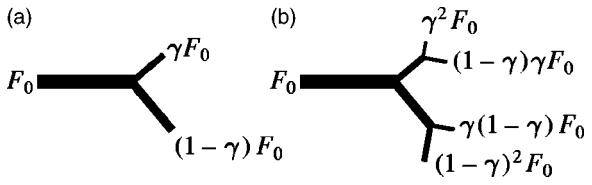

FIG. 4. Asymmetric fractal branching model where fractions γ and $(1-\gamma)$ of total flow F_0 are distributed to daughter branches, shown for (a) one bifurcation and (b) two bifurcations.

microvilli. Separating the hepatocytes and the blood space, is a topologically complex endothelium lining that defines the minute passages of the sinusoids. The fenestrae of the endothelium allow direct access of drug within the circulating plasma to the surface of the hepatocytes via the space of Disse. A very thin but functional and distinct extracellular space of the liver, comprising the space of Disse, exterior to the sinusoid, contains both collagen fibers and ground substance, wherein the microvilli of the hepatocytes extend. Summarily stated, observations of the liver reveal an anatomically unique and complicated structure over a range of length scales designating the space where mibefradil metabolism takes place.

It is the special geometry of the microvascular system that first led researchers to postulate the fractal nature of regional flow networks. The vessels of one generation bifurcate to form vessels of the next generation in a continuous process towards smaller and smaller vessels. Furthermore, the geometry of the daughter branches is not random. Extensive research of the vessels feeding the kidney, lungs, and heart has shown that a scaling relation holds for branch lengths, branch diameters, radius-to-length ratios and intra-arterial pressures [12]. Consequently, the flow into tissues is not randomly distributed among the regional vessels. A distinguishing characteristic of vascular bifurcation is that the two daughters of any generation are asymmetric, with one receiving a fraction γ of the flow and the other a fraction $(1-\gamma)$. Figure 4 shows the results for one and two bifurcations.

This way, the fraction of flow in a given branch can be calculated as a fraction of initial flow F_0, generation number n and flow parameter γ. Here, k takes integer values from 0 to n [28] such that

$$F=\gamma^k(1-\gamma)^{n-k}F_0. \tag{1}$$

The frequency of each value is

$$\frac{n!}{k!(n-k)!} \tag{2}$$

and the mean flow after n generations is

$$\frac{F_0}{2^n}. \tag{3}$$

Simulations carried out with the use of n equal to 15 (which corresponds to 32 768 terminal branches) resulted in distributions that were slightly skewed to the right, which is consistent with experimental data [12]. The discovery and quantification of the fractal nature of regional blood flow has led to new investigations and theories in many areas of anatomy, physiology, and body mechanics. For example, the spatial heterogeneity that exists within isogravitational planes has traditionally been attributed to randomness. The discovery of the fractal nature of the blood vessels, however, indicated that the distribution of flow within an organ may be fractal as well. In fact, this phenomenon has been observed in vessels supplying the lungs, heart, and liver [12,28,29].

By the observations that the liver has a hierarchical structure with complications at many length scales from the order of its macroscopic diameter to the order of the macromolecular makeup of the matrix within the space of Disse, it is hypothesized that the liver is a fractal-like object. That the structure of, and blood flow heterogeneity in, the liver and other visceral organs is fractal, has been suggested and at times experimentally tested before, especially in fields outside of pharmacology and pharmacokinetics [10–12,30,31]. For example, by means of analysis of ultrasonic wave scattering from calf liver tissue, Javanaud [32] measured the fractal dimension of the liver as approximately $d_f \approx 2$ over a wavelength domain of 0.15–1.5 mm. Correspondingly, the liver, as experienced by the drug mibefradil, will be assumed here as being well approximated by a fractal between experimentally relevant length scales [20].

III. IMPLICATIONS OF ORGAN FRACTALITY ON PHARMACOKINETICS

A deeper analysis of the metabolism of mibefradil in the liver requires a description of transport phenomena with chemical reactions in complex media. This can be performed by means of fractal geometry, using two basic exponents: the fractal and spectral dimensions. It must be stressed, however, that a proper level of approximation for reaction-diffusion phenomena in complex fractal media is still an open question.

The application of regional blood flow heterogeneity to pharmacokinetics has resulted in the homogeneous-heterogeneous distribution model developed by Macheras [9], who divided the distribution of drugs in the body into two categories. First, that which occurs under homogeneous (''well stirred'') conditions, and second, that which occurs under heterogeneous (''under stirred'') conditions. The first type of distribution takes place in the upper half of Fig. 5, where the rate of flow is simply F_0. The second type of distribution takes place in the lower half of the diagram, in the deep tissues, where the vascular branching is profuse.

Description of distribution under homogeneous conditions can be done using classical kinetics, while fractal kinetics should be applied to distribution under heterogeneous conditions. Thus the combined, comprehensive model for the distribution of a drug would involve both types of kinetics. Before examining the form of this model, we need to investigate the nature of fractal kinetics.

Classical transport theories, and the resulting mass-action kinetics, applicable to Euclidean structures do not apply to transport phenomena in complex and disordered media. The geometrical constraints imposed by the heterogeneous fractal-like structure of the liver strongly modify diffusional

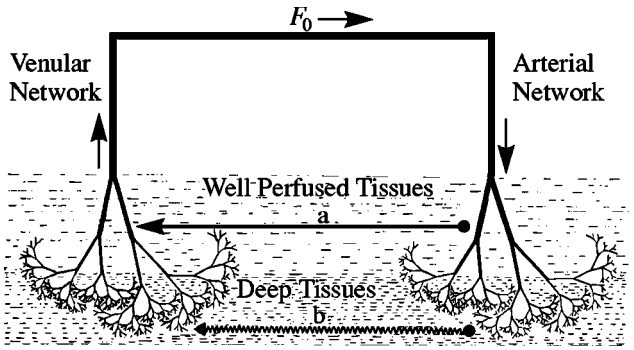

FIG. 5. A complete vascular network used to describe the distribution of drugs in the body. (a) The distribution in well-perfused tissue takes place under homogeneous conditions. (b) The distribution in deep tissue takes place under heterogeneous distribution [9].

dynamics [17]. Topological properties such as connectivity, presence of loops or dead ends, etc., play an important role, hence, it is to be expected that media having different dimensions or even the same fractal dimensions, but different spectral dimensions, could exhibit deviating behavior in diffusional propagation.

Moreover, the statistical probability accounting for the existence of adjacent reactive pairs must be considered. This probability factor is the pair distribution function for the reactive molecules. These two related concerns are addressed in the microscopic concept of an exploration volume of a migrating random walker (drug particle) within the fractal (liver), or otherwise described as the mean number of distinct sites S visited on the fractal at some resolution. A scaling relationship for the spectral dimension that includes S is introduced via [17]

$$S(t) \propto t^{d_s/2}, \tag{4}$$

where time t is proportional to the number of random walk steps, such that that diffusion is monitored by the spectral dimension. Notice that for low spectral dimensions, the random walk will be compact. Subsequently, the macroscopic reaction rate, which is given by the time derivative of $S(t)$, sometimes described as the efficiency of the diffusing, reacting, random walker, will be

$$k(t) \propto \frac{dS(t)}{dt} \propto t^{d_s/2-1} = t^{-(1-d_s/2)} \tag{5}$$

for transient reactions. While strictly valid for low concentrations ($C \rightarrow 0$) as an asymptotic time limit, Eq. (5) is rapidly approximated for realistic concentrations [17]. This time-dependent rate constant, is the manifestation of the anomalous microscopic diffusion in a dimensionally restricted environment leading to anomalous macroscopic kinetics. Consequently, chemical rate laws are a direct reflection of the spatial distribution of particles [18,19] (see Fig. 6). In particular, the classical rate law reflects a random Hertzian distribution, that is one in which the probability of the nearest neighbor of a given particle, to be found at a distance r in a given direction, peaks at $r=0$.

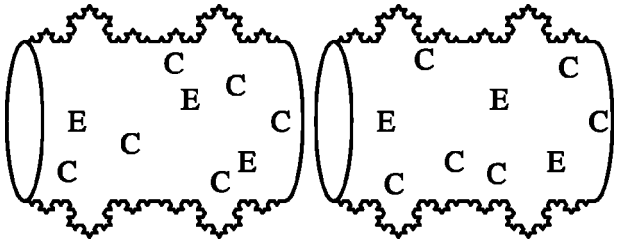

FIG. 6. Two identical fractal containers, with identical macroscopic concentrations of reacting molecules, but with different instantaneous reaction rates. The probability for instantaneous reaction is obviously higher in the container on the left due to the difference in the distribution of substrate molecules.

Heterogeneous reactions taking place at interfaces, membrane boundaries, or within a complex medium such as a fractal when the reactants are spatially constrained on the microscopic level culminate in deviant reaction rate coefficients, that appear to have a sort of temporal memory. The compactness of the low-dimensional random walk implies ineffective diffusion and an entailing aberrant macroscopic rate coefficient. In a fractal-like reaction system the distribution of reactants becomes less random on a mesoscopic scale due to the formation of depletion zones around the traps resulting in a self-ordering or self-unmixing of the reactants around traps—a spontaneous segregation of the reactants occurring at both low and high concentrations [18,19].

The case $d_s=2$ is found to be a critical dimensional value in the phenomena of self-organization of the reactants. For $d_s>2$, the scale of the self-organization is microscopic and independent of time, such that $S(t) \propto t^1$ (is linear) and $k = dS/dt$ is a constant so the reaction kinetics is classical. Below the critical dimension, mesoscopic density fluctuations of the drug become relevant and dependent upon the reaction rate coefficient, whereby S is sublinear of the form in Eq. (4).

If d_s is low (<2), then a random walker (drug) is likely to stay at its original vicinity and will eventually recross its starting point—microscopic behavior conducive to produce mesoscopic depletion zones around traps (enzymes), else, at higher spectral dimensions (>2), a random walker has a finite escape probability—microscopic behavior conducive to rerandomize the distribution of reactants around a trap and replete the supply of reactive pairs, and thus a stable macroscopic reactivity as attested by the classical rate constant [33,34].

The metabolism of mibefradil will be presupposed hereafter to follow the bimolecular annihilating trap reaction within a fractal liver. Furthermore, a constant concentration of a metabolizing enzyme, $E \rightarrow [E]$, is presumed to be present in the liver such that the reaction is expected to have pseudomonomolecular kinetics where only C (the concentration of drug) varies in time. Using Eq. (5), the form of the pseudo-first-order rate coefficient for the metabolism of mibefradil is assumed to be of the power-law form:

$$k(t) = \kappa t^{-(1-d_s/2)} = \kappa t^{-\zeta}, \quad t>1, \quad d_s \leqslant 2, \tag{6}$$

where $\kappa = f(E)$ and is taken to be constant for the experi-

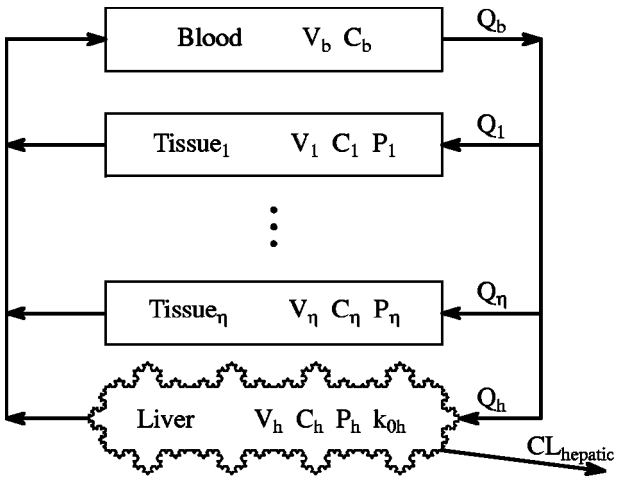

FIG. 7. A simple flow limited physiologically based pharmacokinetic (PBPK) model where clearance of the drug occurs only in the liver by fractal kinetics.

mental data and $\zeta \in [0,1)$ is an unknown parameter to be fitted by the experimental data.

To the best of our knowledge, so far there has not been a paper published explaining the mathematical methods for implementing fractal kinetics nor any other time-dependent kinetic coefficients for pharmacokinetic multicompartmental models. A simple approach for including, within a multicompartmental model, time dependence of the transfer coefficients that vary continuously with the age of human patients was described by Eckerman *et al.* [35], but time dependence was over periods much greater than a single dose. This simplified the mathematics such that there was no time dependence of coefficients for the time course of a single dose. Within a physiological model, over a very long time scale of 98 days, Farris *et al.* [36] introduce time-dependent compartment volume changes due to growth in the studied rat model system. Finally, Macheras [9] introduces the explicit use of time-dependent drug disposition, motivated by the microvascular fractal networks of the body, within what is ostensibly a noncompartmental approach but is mathematically and conceptually equivalent to a one-compartment model.

Presented below is a simple physiologically based pharmacokinetic model (PBPK) [37,38] containing an eliminating compartment with a time-dependent rate of elimination based on fractal kinetics (see Fig. 7).

The total blood flow is defined as

$$Q_b = Q_h + \sum_{i=1}^{\eta} Q_i , \tag{7}$$

where Q_h is the blood flow into the liver and Q_i is the blood flow into a noneliminating tissue. The blood:tissue partition coefficient is taken to be a constant for each compartment, such that $P_i = C_i / C_b$, $i = h,1,\ldots,\eta$. Any drug binding that occurs in the blood or a tissue is assumed to be linear and independent of time, such that $C_b = \mathcal{B} C_f$, where C_f is the concentration of the free unbound drug.

The relevant drug mass balance differential equation for the blood compartment is then

$$\frac{dX_b}{dt} = -Q_b C_b + \sum_{i=1}^{\eta} \frac{Q_i}{R_i} C_i + \frac{Q_h}{R_h} C_h , \tag{8}$$

where X_b is the amount of drug in the blood and C_i, $i = h,1,\ldots,\eta$ are the tissue drug concentrations. The drug mass balance differential equations for the noneliminating tissue compartments are

$$\frac{dX_i}{dt} = Q_i C_b - \frac{Q_i}{R_i} C_i , \tag{9}$$

while for the metabolizing liver compartment

$$\frac{dX_h}{dt} = Q_h C_b - \frac{Q_h}{R_h} C_h - CL_h C_h , \tag{10}$$

where CL_h is the hepatic clearance [39,40].

Consider the pharmacokinetics of the model after an intravenous bolus injection into the blood, such that $X_b(0) = X_b^0 = \text{dose}$ and $X_i(0) = 0 \forall i \neq b$ are the initial conditions of the system. The hepatic clearance is described as $CL_h C_h = k C_h$, provided the metabolism of the drug is a first-order process in C_h as a trap annihilation reaction and k is the first-order rate coefficient. The rate coefficient is assumed to be time dependent of the form $k = k(t) = \kappa t^{-\zeta}$, as a result of the metabolism occurring within a fractal environment, where κ is constant in time and $\zeta \in [0,1)$. Now the mass balance differential equation for the metabolizing liver adopts the form

$$\frac{dX_h}{dt} = Q_h C_b - \left(\frac{Q_h}{R_h} + \kappa t^{-\zeta} \right) C_h . \tag{11}$$

The set of homogeneous linear first-order differential equations may be described with a concise vector notation as

$$\vec{X}' = \mathbb{A}(t)\vec{X}, \quad \vec{X}(0) = \hat{X}, \quad \vec{C} = \mathbb{V}^{-1}\vec{X}, \tag{12}$$

where $\vec{X} = [X_b, X_1, \ldots, X_\eta, X_h]^T$ is a $(\eta+2)$-dimensional column vector of the dependent state variables, $\hat{X} = [X_b^0, 0, \ldots]^T$ is a $(\eta+2)$-dimensional column vector of constants describing the initial conditions, $\mathbb{V} = \delta_{ij} V_i$, $i = b,1,\ldots,\eta,h$, is a constant matrix of the compartment volumes, $\mathbb{A}(t)$ is a matrix describing drug pharmacokinetics with at least one time variable component and $C_i = X_i / V_i$ are compartment concentrations.

Since a system of $(\eta+2)$ first-order equations with at least one variable coefficient is equivalent to a general $(\eta+2)$th-order differential equation, for which exact closed-form solutions exist only rarely when the order is greater than or equal to 2, solutions for Eq. (12) typically remain elusive. Considering that for a PBPK model there may be any natural number η of noneliminating tissues and that the unknown parameter ζ may have a range of fractional values, a general closed-form exact solution is impossible because $\mathbb{A}$ will be a nonconstant matrix of differing sizes. Now, while systems of differential equations may be solved numerically, e.g., by Gear's method for stiff differential equations [41],

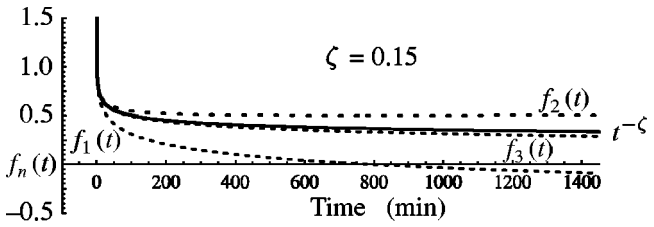

FIG. 8. A comparative graph indicating that the series expansion Eq. (15) rapidly converges over the domain of t spanning the experimental abscissal data for an experimentally relevant value of ζ.

said techniques depend upon input values for all of the parameters, some of which may not be known.

IV. AN APPROXIMATE ANALYTICAL SOLUTION BY PERTURBATION METHODS

If the influences of fractal kinetics in the liver are secondary, as is expected, then ζ will be a small parameter, such that in the limit as $\zeta \to 0$, the familiar classical annihilation kinetics is restored since $\kappa t^{-\zeta} \to \kappa$. With this view, fractal kinetics within the dog model liver can be considered a perturbation of classical kinetics and the solution of the pharmacokinetic system may be assumed to be of the form

$$\vec{X}(t) = \sum_{n=0}^{\infty} \zeta^n \vec{X}_n \tag{13}$$

for the initial conditions $\vec{X}_0(0) = \hat{X}$ and $\vec{X}_n(0) = \hat{0} \forall n \geqslant 1$, where the zero-order term $\vec{X}_0$ fulfills the original initial conditions alone and all terms must submit to the physical boundary condition of $\vec{X}_n(t \to \infty) = \hat{0} \forall n$. Because ζ is a small number, larger powers of ζ and the corresponding higher terms of the above summation are expected to have relatively small magnitudes.

Notice that since ζ is a free parameter independent of t, after a substitution of Eq. (13) into Eq. (12), which gives

$$\sum_{n=0}^{\infty} \zeta^n \vec{X}_n' = \mathbb{A}(t,\zeta) \sum_{n=0}^{\infty} \zeta^n \vec{X}_n, \tag{14}$$

an equivalence of terms for each power of ζ between the left- and right-hand sides of Eq. (14) is implied. But with the coefficient matrix, $\mathbb{A}(t,\zeta)$ containing a term proportional to $t^{-\zeta}$, the aforementioned equivalences are obscured. Using an approach where the recalcitrant term implied by fractal kinetics is approximated as a Maclaurin series expansion in the variable ζ, produces results useful in perturbative methods,

$$t^{-\zeta} = \sum_{n=0}^{\infty} \frac{(-1)^n}{n!} (\ln t)^n \zeta^n = 1 - (\ln t)\zeta + \frac{1}{2}(\ln t)^2 \zeta^2 - \cdots. \tag{15}$$

Importantly, this expansion of $t^{-\zeta}$ is local in ζ (around $\zeta = 0$), but global in t (see Fig. 8). After substitution of the series expansion of $t^{-\zeta}$, the coefficient matrix is obtained as

$$\mathbb{A}(t,\zeta) = \mathbb{A}_0 + \zeta^1 \mathbb{A}_1(t) + \zeta^2 \mathbb{A}_2(t) + \cdots. \tag{16}$$

The substitution of the series form of the coefficient matrix Eq. (16) into Eq. (14) establishes the equivalence of terms for each power of ζ between the left- and right-hand sides, such that

$$\sum_{n=0}^{\infty} \zeta^n \vec{X}_n' = \sum_{n=0}^{\infty} \frac{(-1)^n}{n!} (\ln t)^n \mathbb{A}_n \zeta^n \sum_{n=0}^{\infty} \zeta^n \vec{X}, \tag{17}$$

which leads to the following identities:

$$\begin{aligned}
\zeta^0: &\quad \vec{X}_0' = \mathbb{A}_0 \vec{X}_0, \\
\zeta^1: &\quad \vec{X}_1' = \mathbb{A}_0 \vec{X}_1 + \mathbb{A}_1 \vec{X}_0, \\
\zeta^2: &\quad \vec{X}_2' = \mathbb{A}_0 \vec{X}_2 + \mathbb{A}_1 \vec{X}_1 + \mathbb{A}_2 \vec{X}_0, \\
&\vdots \\
\zeta^n: &\quad \vec{X}_n' = \sum_{i=0}^{\infty} \mathbb{A}_i \vec{X}_{n-i}.
\end{aligned} \tag{18}$$

The zeroth-order perturbation equation from Eq. (18) describing a system of homogeneous first-order linear differential equations, incorporates all of the relevant information of the PBPK model if the drug kinetics within the liver were assumed to be classical. Because $\mathbb{A}_0$ is a matrix with constant coefficients and the initial conditions are known, a solution may be obtained, analogous to a single homogeneous first-order linear differential equation, of the form

$$\vec{X}_0' = \mathbb{A}_0 \vec{X}_0 \wedge \vec{X}_0(0) = \hat{X} \quad \Rightarrow \quad \vec{X}_0(t) = e^{\mathbb{A}_0 t} \hat{X}. \tag{19}$$

After substitution of Eq. (19) into the first-order perturbation equation of Eq. (18), a nonhomogeneous first-order linear differential equation, $\mathbb{A}_1 \vec{X}_0$ being the inhomogeneity, is amenable to solution by the method of variation of parameters

$$\begin{aligned}
&\vec{X}_1' = \mathbb{A}_0 \vec{X}_1 + \mathbb{A}_1 \vec{X}_0, \quad \vec{X}_1(0) = \hat{0} \quad \Rightarrow \vec{X}_1(t) \\
&= e^{\mathbb{A}_0 t} \int e^{-\mathbb{A}_0 t} \mathbb{A}_1(t) \vec{X}_0(t) dt.
\end{aligned} \tag{20}$$

The iterative process of perturbation theory replaces the original intractable differential system Eq. (12) with a sequence of tractable inhomogeneous equations. Generally, the nth-order perturbation equation has a solution based upon the solutions of all the previous perturbation equations, such that

$$\begin{aligned}
&\vec{X}_n' = \sum_{i=0}^{n} \mathbb{A}_i \vec{X}_{n-i}, \quad \vec{X}_n(0) = \hat{0} \\
&\Rightarrow \vec{X}_n(t) \\
&= e^{\mathbb{A}_0 t} \int e^{-\mathbb{A}_0 t} \left(\sum_{i=1}^{n} \mathbb{A}_i(t) \vec{X}_{n-i}(t) \right) dt.
\end{aligned} \tag{21}$$

The final, closed-form analytical description of the proposed PBPK model is established such that

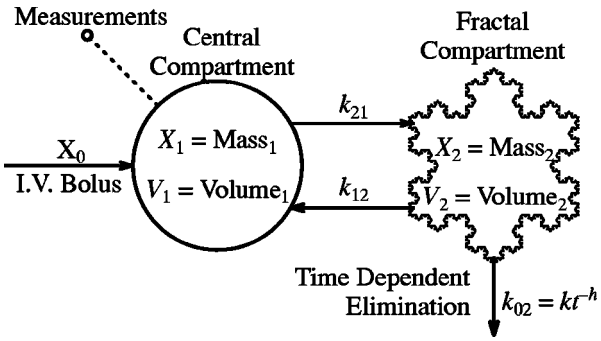

FIG. 9. A diagram of a two-compartment model where the intravenous bolus source enters, and measurements are taken from the central compartment. The secondary compartment is considered fractal with a time-dependent rate of elimination.

$$\vec{X}(t) \approx \vec{X}_0 + \zeta \vec{X}_1 + \zeta^2 \vec{X}_2 + \cdots + \zeta^n \vec{X}_n . \tag{22}$$

By a consideration of the uncertainty of the experimental data, a rational decision regarding the maximum order n of the perturbation terms that is warranted for inclusion may be reached.

V. MODEL PREDICTIONS AND COMPARISON TO EXPERIMENTAL DATA

We intend to subject the method described above to scrutiny by making a direct comparison to experimental data. We assume that the liver is a fractal compartment being the site of elimination of mibefradil and the remaining compartments are Euclidean as shown in Fig. 9.

Here the drug mass balance differential equation for the central compartment is taken to be

$$\frac{dX_1}{dt} = -k_{21}X_1 + k_{12}X_2, \quad X_1(0) = \mathcal{X} = \text{dose}. \tag{23}$$

The drug mass balance differential equation portraying the fractal compartment is

$$\frac{dX_2}{dt} = +k_{21}X_1 - k_{12}X_2 - k_{02}X_2, \quad X_2(0) = 0, \tag{24}$$

where $C_i = X_i / V_i$, k_{21}, and k_{12} are positive first-order transfer rate constants, and k_{02} is an elimination coefficient. The elimination coefficient is assumed to be time dependent as implied by fractal kinetics, such that

$$k_{02} = kt^{-\zeta}, \quad k > 0, \tag{25}$$

where $\zeta \in (0,1]$. Since concentration measurements were drawn from the central compartment, only a solution for that space need be elucidated. By isolating for X_2 in Eq. (23) the following homogeneous second-order linear differential equation with variable coefficients describing the drug concentration in the central compartment is obtained:

$$X_1'' + (k_{21} + k_{12} + kt^{-\zeta})X_1' + k_{21}kt^{-\zeta}X_1 = 0. \tag{26}$$

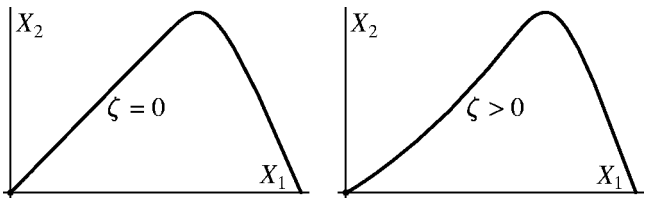

FIG. 10. A numerical plot sketch using experimentally relevant numerical values for the parameters to qualitatively suggest the perturbative effects of fractal kinetics on the trajectory in the phase plane for the model system using Eqs. (23) and (24).

Initial conditions are $X_1(0) = \mathcal{X}$ and by substitution of $X_1(0)$ and $X_2(0)$ into Eq. (23) $X_1'(0) = -k_{21}\mathcal{X}$, while an additional physical requirement is $\lim_{t\to\infty} X_1(t) = 0$. Despite a potential singularity in Eq. (26) at $t = 0$, a phase portrait of the corresponding system of first-order differential equations, Eqs. (23) and (24), indicate a stable trajectory for the solution towards a nodal sink at $t \to \infty$ as yielded by the particular initial conditions for this model (see Fig. 10).

For clarity we change notation where we use ϕ for X_1, a for k_{21}, and b for k_{12}, such that

$$\phi'' + (a + b + kt^{-\zeta})\phi' + akt^{-\zeta}\phi = 0. \tag{27}$$

Since we expect the influences of fractal kinetics in the fractal compartment to be minor corrections, ζ is a small parameter and the solution of the pharmacokinetic system can be assumed in the form

$$\phi(t) = \sum_{n=0}^{\infty} \zeta^n \phi_n(t), \tag{28}$$

such that

$$\phi'(t) = \sum_{n=0}^{\infty} \zeta^n \phi_n'(t) \ \wedge \ \phi''(t) = \sum_{n=0}^{\infty} \zeta^n \phi_n''(t). \tag{29}$$

Following substitutions of terms of the differential equation (27) with the expansions obtained above an equivalence of terms for each power of ζ may be recognized, which yields the identities,

$$\zeta^0: \ \phi_0(0) = \mathcal{X}, \ \phi_0'(0) = -a\mathcal{X},$$

$$\phi_0'' + (a + b + k)\phi_0' + ak\phi_0 = 0,$$

$$\zeta^1: \ \phi_1(0) = 0, \ \phi_1'(0) = 0,$$

$$\phi_1'' + (a + b + k)\phi_1' + ak\phi_1 = k(\ln t)\phi_0' + ak(\ln t)\phi_0, \tag{30}$$

$$\vdots$$

$$\zeta^n: \ \phi_n(0) = 0, \ \phi_n'(0) = 0,$$

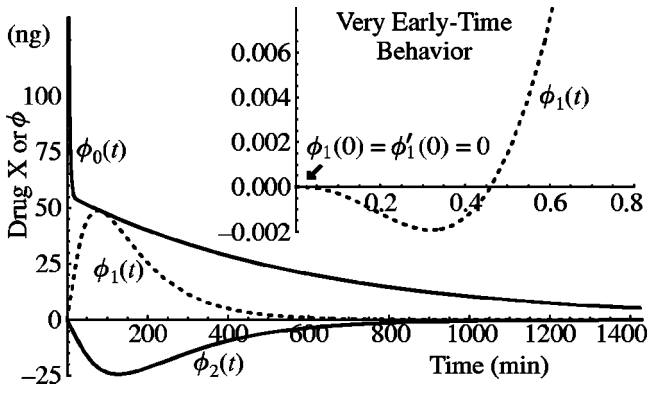

FIG. 11. Comparative graphs of the first three terms impelled by the series of equalities in Eq. (30) for the pharmacokinetic model employing illustrative values of a, b, k, and $\mathcal{X}$. Notice that the initial conditions for the higher-order perturbation terms are met at the origin. The solution implied is $\phi(t) \approx \phi_0(t) + \zeta\phi_1(t) + \zeta^2\phi_2(t)$.

$$\phi_n'' + (a+b+k)\phi_n' + ak\phi_n = \sum_{i=1}^{n} \frac{(-1)^{i+1}}{i!} k(\ln t)^i \left(\frac{d}{dt} + a \right) \phi_{n-i}.$$

The zeroth-order perturbation from Eq. (30), describes a classical two-compartment open model if the elimination kinetics within the secondary compartment were assumed to be classical. The solution is in the form of a sum of exponentials

$$\phi_0(t) = \vartheta_1 e^{s_1 t} + \vartheta_2 e^{s_2 t}, \tag{31}$$

where s_1 and s_2 are negative coefficients that are a function of a, b, and k, while ϑ_1 and ϑ_2 are real coefficients that are functions of a, b, k, and $\mathcal{X}$.

The contributions from the second and all higher-order equations are calculated based on the results under solution in Eq. (31). Success of the method of integration by the variation of parameters used for the postzero terms, depends on integrals of the form

$$I_n = \int (\ln t)^n e^{\theta t} dt, \tag{32}$$

where $\theta(a,b,k)$ is some constant. While these solutions and their derivatives exist, they are expressed in terms of special functions [42]: Euler gamma function $\Gamma(\theta t)$, exponential integral function $Ei(\theta t)$, and the generalized hypergeometric function ${}_pF_q(\overline{\alpha}, \overline{\beta}, \theta t)$.

It is disappointing that the analytical solution to the fractal compartmental model, assembled with the perturbation terms, quickly becomes very complicated because this blunts a touted advantage of this approach. The behaviors of the first three perturbation terms are shown in Fig. 11. Also, the variable ϕ introduced in Eq. (27), may just as well be interpreted as a concentration of the drug in the central compartment for the remainder of this work, since $C_1 = X_1 / V_1$.

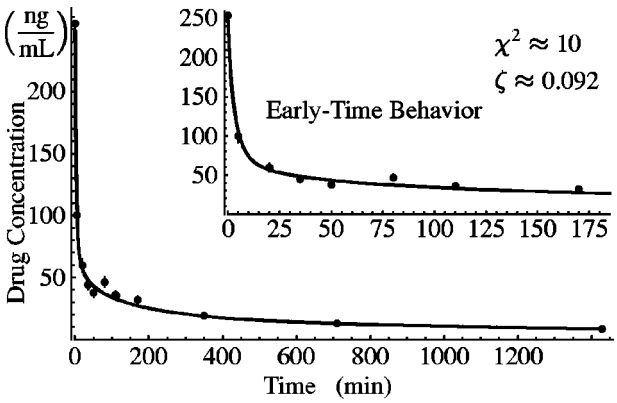

FIG. 12. Mibefradil time course data fit with a three-term perturbation series implied by a two-compartment model with fractal kinetics in the eliminating compartment for trial IV-PV-D2. (Intravenous dose–portal vein sample site–dog 2.)

For a concrete comparison to the experimental data of Ref. [22], a three-term expansion approximation to the solution of the differential equation Eq. (27) was adopted in the form

$$\phi(t) \approx \phi_0(t) + \zeta\phi_1(t) + \zeta^2\phi_2(t), \quad \zeta \ll 1, \tag{33}$$

and compared to the pharmacokinetic data using the techniques of nonlinear fits with a global optimization method (see Fig. 12). The best-fit values for the small parameter ζ were $\zeta_{D1} = 0.084$, $\zeta_{D2} = 0.092$, $\zeta_{D3} = 0.111$, and $\zeta_{D4} = 0.043$, for dogs numbered 1–4, respectively. The absolute discrepancies estimated by the chi-squared function are $\chi^2_{D1} \approx 17$, $\chi^2_{D2} \approx 10$, $\chi^2_{D3} \approx 14$ and $\chi^2_{D4} \approx 23$.

Because the pharmacokinetic model Eq. (28) is nonlinear with respect to the unknown parameters, to establish the variance of the fitted small parameter, ζ, synthetic sets of data via Monte Carlo methods were fabricated. While a standard bootstrap approach [43] is based upon resampling methods whereby sets of N data points are randomly selected with replacement from the original set of data, ${}^0\vec{Z}$, this technique is troublesome for the pharmacokinetic data studied here. Since the data sets (see Fig. 13) are rather small and with a particular lack of sampling at early times when rapid changes in concentration occur, and a data set missing influential data points would prejudice calculations, synthetic data sets more reflective of the experimental data sets were devised. A Gaussian distribution centered at each point in ${}^0\vec{Z}$, with a standard deviation, $\sigma_i = 0.09 C_i$, $i = 1, \ldots, N$, allows for new data sets, still possessing the inherent uncertainties but without duplications or omissions, to be created.

A practically manageable number, $N = 300$, of synthetic data sets, ${}^i_S\vec{z}$, $i = 1, \ldots, N$, were pseudorandomly generated by computer for each dog data set and fit. A resulting M-dimensional distribution of fitted parameters, ${}^i_S\vec{a}$, $i = 1, \ldots, N$, corresponding to different chi-squared values can be observed over one intersecting plane in Fig. 14. The one-dimensional confidence intervals for the parameters are indicated by the appropriate projections of the region onto the axes.

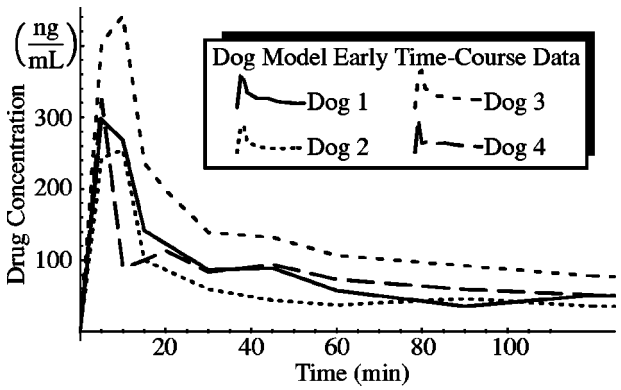

FIG. 13. An inspection of the very early time behavior of the concentration time-course data for each dog indicating the initial increase in drug concentration occurs over a shorter time than the resolution of the experiment.

The best-fit values for the small parameter, ζ, including uncertainties, were: $\zeta_{D1}=0.084\pm0.020$, $\zeta_{D2}=0.092\pm0.014$, $\zeta_{D3}=0.111\pm0.016$, and $\zeta_{D4}=0.043\pm0.028$, for dogs 1–4, respectively. This implies, by Eq. (6), that the calculated values of the spectral dimension for each of the dog livers are: $d_s^{D1}=1.832\pm0.040$, $d_s^{D2}=1.816\pm0.028$, $d_s^{D3}=1.778\pm0.032$, and $d_s^{D4}=1.914\pm0.056$. A quick comparison indicates that there is near agreement amongst all of the results to within experimental and theoretical uncertainty.

VI. DISCUSSION AND CONCLUSIONS

In this paper we presented an approach to the base pharmacokinetics in a multicompartment system by including the presence of a fractal organ. We have argued that the liver, where most of the enzymatic processes of drug elimination take place, has a fractal structure. Hence, we expect transport processes as well as chemical reactions taking place in the liver to carry a signature of its fractality. A general PBPK model was proposed and elucidated incorporating at least one heterogeneous component following fractal kinetics. After a local series expansion of the time-dependent rate constant around $\zeta=0$, assuming that the fractal effects on the time-dependent rate constant were small, approximate analytic solutions to the model, differential mass balance equations were derived by perturbative techniques. As a concrete application of our methodology, the pharmacokinetics of mibefradil in a dog model system was scrutinized.

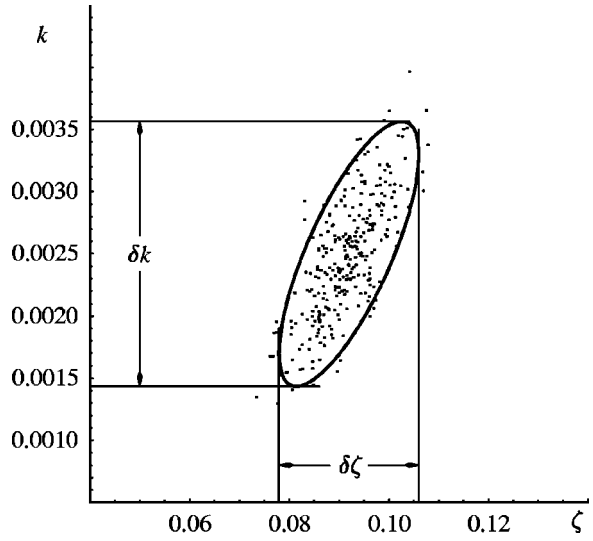

FIG. 14. The confidence region intersecting the k-ζ plane in parameter space for trial IV-PV-D2, indicating an ellipse of 90% confidence.

Since the physiology of the liver supported the hypothesis that mibefradil may experience a fractal-like environment within, fractal kinetic theory suggested the adoption of a time-dependent rate constant, with power-law form, determined by the spectral dimension.

Mibefradil concentration-time course data were analyzed with a mathematically analogous multicompartment model with the goal of measuring the effective spectral dimension of the dog liver. Estimates were: $d_s^{D1}=1.832\pm0.040$, $d_s^{D2}=1.816\pm0.028$, $d_s^{D3}=1.778\pm0.032$, and $d_s^{D4}=1.914\pm0.056$, for the four dog data sets, though these results are not enthusiastically endorsed by the chi-squared test statistic for the adopted experimental uncertainty. Yet, it is proffered that heterogeneous processes of drug distribution and reaction in the liver can obey principles of fractal kinetics. The values of the fractal dimension obtained through this analysis are consistent with the ultrasound experiment results of $d_f=2.0$.

To account for the observed experimental deviations we comment that the adopted experimental uncertainty of 9% was likely to be too conservative or that it was not normally distributed. Indeed, a further consideration of the uncertainties of the data is warranted. For example, since the slope is so steep during the initial peak phase of the experiment, $t<25$ min, even small uncertainties in the measurement times, which we assumed to be zero, would produce large uncertainties in the concentration measurements. Additionally, the intrinsic uncertainties of the biological model systems are likely to produce outlying data points that conspire to indicate low goodness-of-fit tests. This lack of predictability may arise from different sources; these include system instability, environmental fluctuations due to effects outside of the systems modeled, and measurement uncertainties. Besides containing mundane signal and noise, irregular time series may be chaotic—irregularities produced by the intrinsic deterministic dynamics of a nonlinear biological system [44]. The least-squares fitting, linear or nonlinear, is a maximum likelihood estimation of the fitted parameters, if the measurement errors are independent and Gaussian distributed and may not have been ideal for the data sets used. Perhaps a reanalysis of the data is justified within the context of robust statistics—statistics that are less sensitive to noise within the data [45–48].

Considering that this paper favors the interpretation that the kinetics of mibefradil are affected by the fractal structure of the liver that consequently reduces the rate of metabolism and clearance of drug over time, the question of why nature would design the liver in such a way is raised. Now while there is no performance advantage over a well stirred, classically imagined compartment, one with a rate constant due

to a uniformly random distribution of drug and enzyme, such a compartment may well be impossible to achieve under biological designs and the implied comparison is therefore an ill posed one [49]. It may be that the fractal liver design is the best design possible, such that comparisons against nonideal theoretical models, as a poorly stirred sphere with enzymes adhered along the inner wall, are favorable. For example, the fractal structure, with many layers of membrane at its interface, allows the organ to possess a high number (concentration) of enzymes, thus giving it a high reaction rate despite time-dependent (decay) fractal kinetics. Indeed, the intricate interlacing of a stationary, catalytic phase of hepatocytes with a liquid phase of blood along a fractal border is what reduces the required diffusional distances for reactions to take place with any appreciable celerity. Moreover, the complicated structure of the liver, which provides for a huge interface between drug and hepatocytes, may be generated quite simply during the growth of the liver. The fractal form may be parsimoniously encoded in the DNA, indirectly specified by means of a simple recursive algorithm that instructs the biological machinery in how to construct the liver. In this way, a vascular system made up of fine tubing with an effective topological dimension of one may fill the three-dimensional embedding space of the liver. These possibilities reveal that the structure of the liver may be necessarily that of a fractal.

This possibility would not be out of line with other examples of optimization in biological design. In fact, a hypothesis has been put forward, called the hypothesis of symmorphosism which states that biological systems achieve a state of structural design commensurate to functional needs resulting from regulated morphogenesis such that the formation of structural elements satisfies, but does not exceed the requirements of the functional system [50,51]. Examples to support this hypothesis have been discussed, which range from enzyme systems and muscle cells, to the nervous system and the respiratory system [52,53]. It is quite plausible that the liver design is optimized for the elimination of toxic substances through effecient enzyme action on a fractal object.

ACKNOWLEDGMENTS

The authors express gratitude to Dr. Y. K. Tam for making the data sets from his experiments available for our study. Useful discussion with Dr. Y. K. Tam and Dr. D. Ridgway of Kinetana Inc. are gratefully acknowledged. The assistance and advice of Dr. S. R. Lele in the statistical data analysis is much appreciated. This research was supported by NSERC and MITACS as part of the project ''Mathematical Modelling and Pharmaceutical Development.''

[1] E. Gladtke and H.M. von Hattingberg, *Pharmacokinetics: An Introduction* (Springer-Verlag, Berlin, 1979).
[2] M.E. Winters, *Basic Clinical Pharmacokinetics* (Applied Therapeutics, Vancouver, Washington, 1994).
[3] M. Gibaldi and D. Perrier, *Pharmacokinetics*, 2nd ed. (Dekker, New York, 1982).
[4] T.L. Schwinghammer and P.D. Kroboth, J. Clin. Pharmacol. **28**, 388 (1988).
[5] R.H. Levy and L.A. Bauer, Ther. Drug Monit **8**, 47 (1986).
[6] J.J. DiStefano and E.M. Landaw, Am. J. Physiol. **246**, R651 (1984).
[7] W.A. Colburn *et al.*, J. Clin. Pharmacol. **28**, 879 (1988).
[8] W.R. Gillespie, Clin. Pharmacokinet **20**, 243 (1991).
[9] P. Macheras, Pharm. Res. **13**, 663 (1996).
[10] J. B. Bassingthwaighte, L. Liebovitch, and B. West, *Fractal Physiology* (Oxford University Press, New York, 1994).
[11] *Fractals in Biology and Medicine*, edited by T. Nonnenmacher, G. Losa, and E. Weibel (Birkhäuser Verlag, Basel, 1994).
[12] J.B. Bassingthwaighte, R.B. King, and S.A. Roger, Circ. Res. **65**, 578 (1989).
[13] M.A. Weiss, J. Theor. Biol. **184**, 1 (1997).
[14] K.M. van der Graff and S.I. Fox, *Concepts of Human Anatomy and Physiology*, 2nd ed. (W. M. C. Brown, Iowa, 1988).
[15] B.J. West and A.L. Goldberger, Am. Sci. **75**, 354 (1987).
[16] M. Giona, Chem. Eng. Sci. **47**, 1503 (1992).
[17] S. Havlin and D. Ben-Avraham, Adv. Phys. **36**, 695 (1987).
[18] R. Kopelman, J. Stat. Phys. **42**, 185 (1986).
[19] R. Kopelman, Science **241**, 1620 (1988).
[20] H. Koch, Pharmazie **48**, 643 (1993).
[21] E. Ragazzi, Pharmazie **50**, 66 (1995).
[22] A. Skerjanec, S. Tawfik, and Y.K. Tam, J. Pharm. Sci. **85**, 189 (1995).
[23] H. Wiltshire, B. Sutton, G. Heeps, A. Betty, D. Angus, S. Harris, E. Worth, and H. Welker, Xenobiotica **27**, 557 (1997).
[24] H.A. Welker, J. Pharm. Pharmacol. **50**, 983 (1998).
[25] J.L. Campra and T.B. Reynolds, in *The Liver: Biology and Pathobiology*, edited by I.M. Arias, H. Popper, D. Schachter, and D.A. Shafritz, 1st ed. (Raven Press, New York, 1982).
[26] W.W. Loutt and M.P. Macedo, Drug Metab. Rev. **29**, 369 (1997).
[27] H. Elias, in *The Liver: Morphology, Biochemistry, Physiology*, edited by C. Rouiller (Academic Press, New York, 1963), Vol. I.
[28] R.W. Glenny and H.T. Robertson, J. Appl. Physiol. **69**, 532 (1990).
[29] R.W. Glenny and H.T. Robertson, J. Appl. Physiol. **70**, 1024 (1991).
[30] M. Sernetz, J. Wubbeke, and P. Wlczek, Physica A **191**, 13 (1992).
[31] B. B. Mandelbrot, *The Fractal Geometry of Nature* (Freenan, San Francisco, 1977).
[32] C. Javanaud, J. Acoust. Soc. Am. **86**, 493 (1989).
[33] Y.-E. Koo and R. Kopelman, J. Stat. Phys. **65**, 185 (1986).
[34] R. Kopelman, A. Lin, and P. Argyrakis, Phys. Lett. A **232**, 34 (1997).
[35] K.F. Eckerman, R.W. Leggett, and L.R. Williams, Radiat. Prot. Dosim. **41**, 257 (1992).
[36] F. Farris, R. Dedrick, P. Allen, and J. Smith, Toxicol. Appl. Pharmacol. **119**, 74 (1993).

[37] M.R. Rowland and A.M. Evans, in *New Trends in Pharmacokinetics*, Vol. 221 of *NATO Advanced Study Institute, Series A: Life Sciences*, edited by Aldo Resagno and Ajit K. Thakur (Plenum Press, London, 1992), pp. 83–115.
[38] K.-C.T. Hoang, Toxicol. Lett. **79**, 99 (1995).
[39] H. Boxenbaum, Drug Metab. Rev. **24**, 89 (1992).
[40] L. Gerlowski and R. Jain, J. Pharm. Sci. **72**, 1103 (1983).
[41] R. Redheffer, *Differential Equations: Theory and Applications* (Jones & Barlett, Boston, 1991), Chap. 17.
[42] I. Gradsteyn and I. Ryzhik, *Table of Integrals, Series, and Products*, 5th ed. (Academic Press, New York, 1994).
[43] J.R. Taylor, *An Introduction to Error Analysis: The Study of Uncertainties in Physical Measurements* (University Science Book, Mill Valley, 1982).
[44] D.W.A. Bourne, *Mathematical Modeling of Pharmacokinetic Data* (Technomic Publishing Company, Lancaster, Pennsylvania, 1995).
[45] G.A. Milliken and D.E. Johnson, *Analysis of Messy Data*, (Chapman and Hall, London, 1992), Vol. I.
[46] D.C. Hoaglin, F.M. Mosteller, and J.W. Tukey, *Understanding Robust and Exploratory Data Analysis* (Wiley, New York, 1983).
[47] P.J. Rousseeuw and A.M. Leroy, *Robust Regression and Outlier Detection* (Wiley, New York, 1987).
[48] A. Atkinson and M. Riani, *Robust Diagnostic Regression Analysis* (Springer-Verlag, New York, 2000).
[49] E. Liang and H. Derendorf, J. Pharmacokinet Biopharm. **26**, 247 (1998).
[50] B.J. West and B. Deering, in *The Lure of Modern Science*, edited by B.J. West, B. Deering, Bill Deering, and W. Deering, Studies of Nonlinear Phenomena in Life Science Vol. 3 (World Scientific, New Jersey, 1995).
[51] E.R. Weibel, C.R. Taylor, and H. Hoppeler, Proc. Natl. Acad. Sci. U.S.A. **88**, 10357 (1991).
[52] E.R. Weibel, *The Pathway for Oxygen* (Harvard University Press, Cambridge, Massachusetts, 1984).
[53] E.R. Weibel, *Symmorphosis* (Harvard University Press, Cambridge, Massachusetts, 2000).